

Design of new fluorinated bridged push–pull stilbenes and preparation of LB films for second harmonic generation in the blue domain†

Stéphanie Desrousseaux,^a Bernard Bennetau,^a Jean-Pierre Morand,^b Christophe Mingotaud,^c Jean-François Létard,^{*d} Sébastien Montant^e and Eric Freysz^e

^a Laboratoire de Chimie Organique et Organométallique (CNRS UMR 5802), Université de Bordeaux I, 351 Cours de la Libération, F-33405 Talence cedex, France

^b Laboratoire d'Analyse Chimique par Reconnaissance Moléculaire, Ecole Nationale Supérieure de Chimie et de Physique de Bordeaux, Av. Pey-Berland BP 108, F-33402 Talence, France

^c Centre de Recherche Paul Pascal, Av. du Docteur A. Schweitzer, F-33600 Pessac, France

^d Laboratoire des Sciences Moléculaires, Institut de Chimie de la Matière Condensée de Bordeaux (CNRS UPR 9048), Université de Bordeaux I, Av. du Docteur A. Schweitzer, F-33608 Pessac, France. E-mail: Letard@chimsol.icmcb.u-bordeaux.fr

^e Centre de Physique Moléculaire Optique et Hertzienne (CNRS UMR 5798), Université de Bordeaux I, 351 Cours de la Libération, F-33405 Talence, France

Received (in Montpellier, France) 22nd June 2000, Accepted 9th October 2000

First published as an Advance Article on the web 21st November 2000

In order to prepare alternating Y-type multilayers involving push–pull stilbenes giving second harmonic generation (SHG) in the blue domain, we have synthesized two new bridged compounds, **1** and **2**, with the hydrophobic chain grafted onto the donor group. The photophysical properties of these dyes in both solution and LB films are reported. The SHG signal of monolayer LB films containing **1** and **2** are close to that of the analog **3** and **4** having the hydrophobic chain grafted onto the acceptor group. Finally, multilayer LB films based on one, two and four bilayers of **1/3** or **2/4** were prepared and the SHG measurements show a regular noncentrosymmetric arrangement for **2/4** films only.

During the last few decades the potential development of optoelectronic devices, based on nonlinear optical processes induced in molecular materials, has attracted considerable attention.^{1–5} It is now well-known that organic materials exhibit higher efficiency than inorganic compounds as far as second-order nonlinear optical (SONLO) properties are concerned. Moreover, in addition to the wide range of active molecules, the processability of such materials is considerably improved, making them all the more attractive.^{4–6}

On the basis of a two-state model,¹ it has been suggested and experimentally confirmed that conjugated systems substituted by donor–acceptor groups exhibit large optical responses. In the blue spectral region, the push–pull stilbenes represent an important class of fluorescent dyes.^{7,8} The photophysical and photochemical properties of these compounds are very appealing because of their particularly strong charge transfer in the excited state.^{9,10} Nevertheless, increasing the strength of the donor–acceptor groups induces a red-shift of the absorption spectrum⁷ and therefore limits the applications in the blue domain. Ulman *et al.*⁸ showed that a $-\text{SO}_2^-$ group, which is a strong σ -acceptor, induces a lower absorption red-shift than the π -acceptor $-\text{NO}_2$ group, despite similar σ_p and σ^- values.¹¹ In addition, the ability of stilbene molecules to form H-aggregates in Langmuir–Blodgett (LB) films,^{12,13} which are characterized by a hypsochromic absorption shift,¹⁴ emphasises the interest in such sulfonyl stilbenes as good candidates for SONLO response in the blue domain. Along these lines, Le Breton *et al.*^{15,16} have synthesized some bridged derivatives of polyphilic stilbenes (**3** and **4**, see Fig. 1). The central double bond has been incorporated into a five-

membered ring in order to reduce photochemical processes.¹⁷ The hydrophobic long perfluoroalkyl ($-\text{C}_8\text{F}_{17}$) chain was selected because of its self-assembling property, observed when the perfluoroalkyl chain is longer than heptane.¹⁸

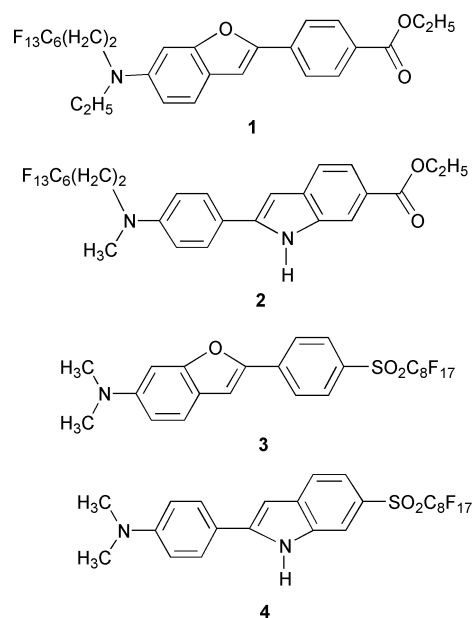


Fig. 1 Molecular structure of **1–4**: **1** = 4-[6-[ethyl(1*H*,1*H*,2*H*,2*H*-perfluorooctyl)amino]benzofuran-2-yl]benzoic acid ethyl ester; **2** = 2-[4-[methyl(1*H*,1*H*,2*H*,2*H*-perfluorooctyl)amino]phenyl]-1*H*-indole-6-carboxylic acid ethyl ester; **3** = 2-(4'-heptadecafluorooctylsulfonylethyl)-6-(*N,N*-dimethyl)aminobenzofuran and **4** = 2-[4'-(*N,N*-dimethyl)aminophenyl]-6-heptadecafluorooctylsulfonylethylindole.

† This paper is dedicated to the memory of Olivier Kahn.

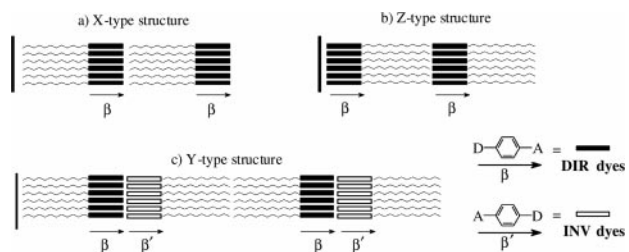


Fig. 2 Display of X- and Z-type structures of LB multilayers ((a) and (b)). Alternating layers of 1–4 molecules when deposited in a Y-type configuration (c).

Monolayer LB films of **3** and **4** have been prepared and the SONLO response from the surface set-up gave a molecular quadratic hyperpolarizability β of 200×10^{-30} esu.¹⁶

The LB technique is a widely developed method for building ordered arrays of molecules, in particular as a means of imposing the non-centrosymmetric structure necessary to the generation of a second harmonic response at the macroscopic level. Nevertheless, most compounds adopt centrosymmetric head-to-head or tail-to-tail arrangements (Fig. 2). It is necessary to alternate the optically active layers with inactive spacers,¹⁹ or to include interdigitating arrangements^{20,21} or to deposit two different active molecules.²² Each species is alternatingly deposited, the hydrophobic chain being grafted onto the acceptor of the first species (DIR) and the donor group of the second species (INV). The nonlinear susceptibility resulting from the addition of the individual nonlinearities of each monolayer is expected to be quite large, with the additional advantage of a high degree of order and a better stability of the structure.

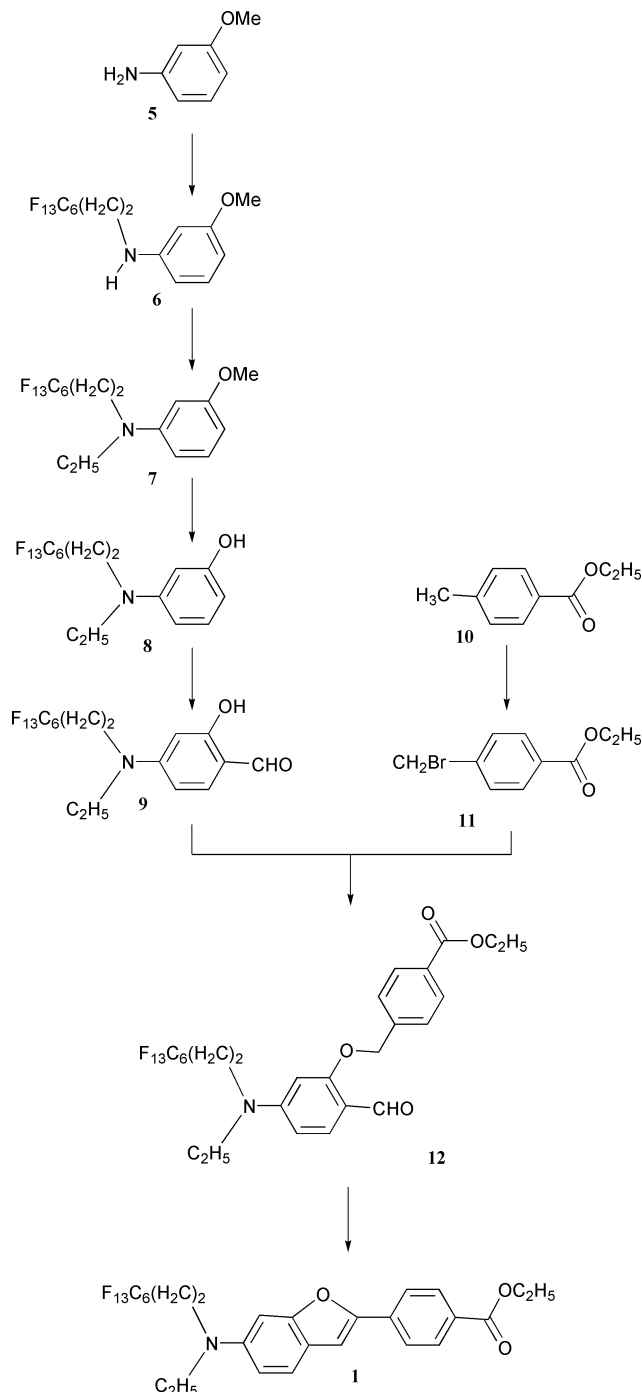
In this work, we describe the preparation of alternating Y-type multilayers involving push–pull stilbenes with second harmonic generation in the blue domain. We present the synthesis of two new bridged stilbenes, **1** and **2** (Fig. 1), which are the analogs of **3** and **4** having the hydrophobic chain grafted onto the donor group. The photophysical properties of **1** and **2** were studied both in solution and in LB films. The SONLO responses using SHG-surface technique are firstly reported for LB films containing only the **1** and **2** dyes. Alternating layers of **1/3** and **2/4** were also prepared and their SONLO properties are described.

Results and discussion

Synthesis of compounds **1** and **2**

1 and **2** are two new polyphilic compounds with an ester hydrophilic head, a stilbene rigid core and a hydrophobic fluorinated chain. In these molecules, the central double bond is incorporated in a five-membered ring in order to prevent *trans*–*cis* photoisomerization.^{15–17} A spacer containing two carbon atoms is introduced between the perfluorinated chain and the amino group in order to reduce the influence of the electronic effect of fluorine atoms on the donor capacity of the nitrogen atom. The weak acceptor ester group is selected in order to obtain a good transparency in the blue domain.

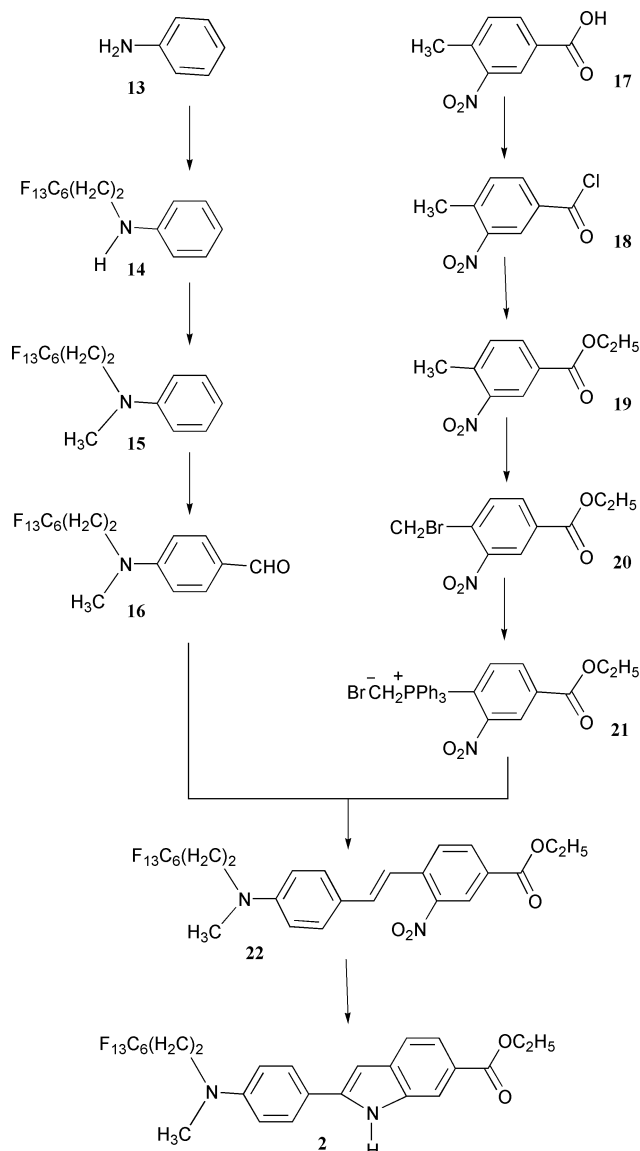
1 was synthesized according to the multi-step pathway described on Scheme 1. Both the perfluorinated chain and the spacer were introduced on the donating moiety during the first step by nucleophilic substitution between $C_6F_{13}(CH_2)_2I$ and *m*-anisidin **5**, an excess of this amine leading to the secondary amine **6** as the only substituted product. The tertiary amine **7** was synthesized by ethylation of **6** under basic conditions. The hydroxyl group of **8** was released by the deprotection method using BBr_3 in dichloromethane; 2 equiv. of BBr_3 were necessary because boron atoms complex both oxygen and nitrogen. The amino phenol compound **8** was mono-



Scheme 1 Route followed for the synthesis of **1**.

formulated at the *para* position to the amino group with *N,N*-dimethylformamide and phosphorus oxychloride; this Vilsmeier–Haack reaction^{23,24} afforded the aldehyde **9**. Particular experimental conditions (see Experimental) prevented the formation of the product diformylated at the *para* positions to the amino and hydroxyl groups. Starting from compound **10**, the withdrawing moiety of dye **1** was obtained by radical benzylic bromination with *N*-bromosuccinimide to yield the brominated ester **11** as the major product of the reaction. An ether bridge was then created between the donating **9** and the withdrawing **11** moieties by nucleophilic substitution under basic conditions.²⁵ Benzofuran derivative **1** was finally obtained by an intramolecular Knoevenagel reaction on **12** using alumina-supported potassium fluoride;²⁶ in spite of the strong character of this base, anhydrous conditions prevented the hydrolysis of the ester function.

The synthesis of **2** was performed following the pathway shown on Scheme 2. The introduction of the fluorinated



Scheme 2 Route followed for the synthesis of 2.

hydrophobic tail was realized as described for the preparation of compound 6, using aniline 13²⁷ as the nucleophilic reagent instead of *m*-anisidin 5. The secondary amine 14 was then methylated under basic conditions to give the tertiary amine 15. The donating moiety 16 was finally obtained by formylation at the *para* position using the Vilsmeier–Haack reaction. Starting from the disubstituted benzoic acid 17, the withdrawing moiety of 2 was synthesized according to the following procedure. The ester derivative 19 was obtained in a one-pot reaction by first forming the acid chloride compound

18 with an excess of thionyl chloride and then performing an alcoholysis with absolute ethanol. Compound 19 was afterwards submitted to a radical bromination with *N*-bromosuccinimide to give the brominated ester derivative 20 as the major product. Finally, the phosphonium salt 21 was obtained by reaction between triphenylphosphine and the bromobenzyl derivative 20. The *trans*-stilbene 22 was obtained by a Wittig reaction²⁸ involving the donating 16 and the withdrawing 21 moieties under basic conditions. The indolic derivative 2 was obtained in the last step by cyclization of the stilbene with an excess of triethyl phosphite, probably according to a mechanism described by Sundberg.²⁹

Absorption and emission properties in solution

The absorption maxima measured in solvents of increasing polarity are reported in Table 1. A small bathochromic shift of the longest wavelength band is observed from *n*-hexane to acetonitrile, suggesting that the Franck–Condon electronic excitation involves a relatively small charge transfer. It is worth noting that even in polar solvent the absorption maxima never exceed 390 nm for 1 and 362 nm for 2. This result is important for designing SONLO materials in the blue domain.

The fluorescence maxima are reported in Table 1 as a function of the solvent polarity. Fig. 3 shows the fluorescence spectra of 2 in *n*-hexane, diethyl ether and dimethylformamide. In nonpolar and strongly polar solvents (for 2) and in polar solvents only (for 1) the spectra are structureless. The position of the fluorescence maxima ($\lambda_{\text{fluo}}^{\text{max}}$) is strongly red-shifted from *n*-hexane to acetonitrile, indicating a larger dipole moment in the excited state than in the ground state. The dipole moment of the excited state (μ_e) can be determined by the solvatochromic method. The equations to calculate μ_e were first derived by Ooshika,³⁰ Lippert,³¹ Liptay³² and Mataga *et al.*³³ All are

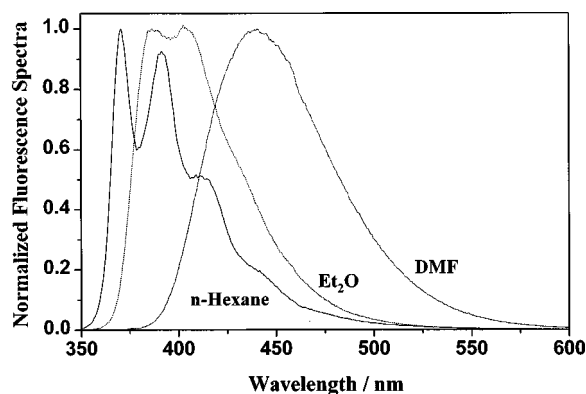


Fig. 3 Normalized fluorescence spectra of 2 at room temperature in *n*-hexane ($\Delta f' = 0.092$), diethyl ether (Et_2O , $\Delta f' = 0.256$) and dimethylformamide (DMF, $\Delta f' = 0.378$).

Table 1 Absorption ($\lambda_{\text{abs}}^{\text{max}}$) and fluorescence ($\lambda_{\text{fluo}}^{\text{max}}$) maxima, fluorescence quantum yields (ϕ_f), lifetimes (τ_f) and radiative (k_r) and non-radiative (k_{nr}) rate constants in solvents of different polarity at room temperature

Compound	Solvent	$\lambda_{\text{abs}}^{\text{max}}/\text{nm}$	$\lambda_{\text{fluo}}^{\text{max}}/\text{nm}$	ϕ_f	τ_f/ns	$k_r/10^9 \text{ s}^{-1}$	$k_{\text{nr}}/10^7 \text{ s}^{-1}$
1	<i>n</i> -Hexane	369	398	0.39			
	BuOMe	374	451	0.32			
	EtO ₂	374	444.5	0.44	2	0.2	25
	THF	382	479	0.32			
	DMF	390	525	0.42			
	CH ₃ CN	384	524	0.44	2.8	0.2	25
2	<i>n</i> -Hexane	347	370	0.38	1.2	0.3	49
	BuOMe	352	389	0.42			
	EtO ₂	351	386	0.47	1.3	0.4	45
	THF	355	410	0.54			
	DMF	362	440	0.47			
	CH ₃ CN	356	440	0.47	1.6	0.3	34

based on the Onsager description of a solute-induced reaction field inside a spherical solvent cavity of radius ρ .³⁴ This parameter is estimated from the molecular volume calculated from the molecular weight and density of ethyl benzoate (1.051 g cm⁻³). With the usual assumptions,^{35,36} the excited state dipole moment (μ_e) is given by eqn. (1):

$$\bar{\nu}_{\text{fluo}}^{\text{max}} = -2\mu_e(\mu_e - \mu_g)\Delta f'/hc\rho^3 + \text{Const} \quad (1)$$

The polarity parameter $\Delta f'$ is defined by $[(\epsilon - 1)/(\epsilon + 1)] - 0.5[(n^2 - 1)/(2n^2 + 1)]$ where ϵ and n are the dielectric constant and the optical refractive index, respectively. The solvatochromic slopes determined by the plot of fluorescence maxima ($\bar{\nu}_{\text{fluo}}^{\text{max}}$) vs. $\Delta f'$ are gathered in Table 2. The dipole moment of the ground state (μ_g) has been calculated, in a first approximation, by the semi-empirical AM1 method.³⁷ The resulting μ_e values are listed in Table 2 and compared to those of compounds **3** and **4**. Note that these values are only approximate because of (i) the rough evaluation of ρ and (ii) the nonlinearity of the bridged compounds, which may induce different orientations of the dipole moment for the ground and excited states. Nevertheless, these data show that **1–4** possess large excited state dipole moments. Moreover, the change of the dipole moment between the ground and the excited states ($\Delta\mu_{eg}$) is larger for **1** and **2** than for **3** and **4** due to the smaller ground state dipole moments associated with the ester acceptor group.

The fluorescence quantum yields (ϕ_f) of **1** and **2** in different solvents are collected in Table 1. Fig. 4 shows the plot of ϕ_f as a function of the solvent parameter $\Delta f'$ for **1–4**. The fluorescence quantum yields of **1** and **2** are not significantly affected by the solvent polarity and remain around 0.4, whatever the solvent polarity, whereas for **3** and **4** a strong decrease occurs in polar solvents.¹⁷ Let us recall that push-pull stilbenes, like 4-*N,N*-dimethylamino-4'-cyano stilbene (DCS),^{38–40} are strongly altered in their photophysical properties by the flexibility or non-flexibility of their single and double bonds. In DCS, double bond twisting leads to fluorescence quenching (state P*), whereas twisting the adjacent single bonds populates lower-lying emissive charge transfer states (A*, twisted intramolecular charge transfer, TICT),⁴¹ which competes with

Table 2 Solvatochromic slope m [cm⁻¹ ($\Delta f'$)⁻¹] using the data of Table 1, Onsager parameter (ρ) and ground (μ_g) and excited (μ_e) state dipole moments

	1	2	3	4
Slope m	-20 890	-15 050	-20 610	-18 160
$\rho/\text{g cm}^{-3}$	6.28	6.23	6.11	6.10
μ_g/D	3.1	2.5	6.5	6.5
μ_e/D	24	20	24	23

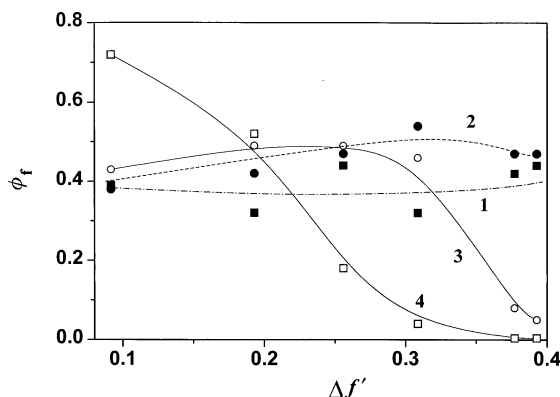


Fig. 4 Fluorescence quantum yields as a function of solvent for (■) **1**, (●) **2**, (○) **3** and (□) **4**.

fluorescence quenching (state P*) and therefore raises the fluorescence quantum yield.⁴⁰ When the central double bond is chemically bridged in a five-membered ring⁴⁰ the P* state is not available. In bis-donor stilbenes, the quantum yield of fluorescence remains high whatever the solvent polarity.⁴² In push-pull stilbenes with a strong acceptor group, like a nitro⁴³ or a pyridinium ion,^{44,45} the fluorescence quantum yield falls in polar solvents as a result of TICT state formation with non-emissive character. For **3** and **4** bearing a strong acceptor substituent ($-\text{SO}_2\text{C}_8\text{F}_{17}$), we effectively demonstrated the presence of a non-emissive TICT state in polar solvent and then explained the decrease of ϕ_f in polar solvents.¹⁷ For **1** and **2**, the ϕ_f values remain nearly solvent-independent (Fig. 4). Moreover, the fluorescence decays (τ_f) measured at room temperature (Table 1) and satisfactorily fitted by a single-exponential model, are relatively independent of the solvent polarity. Similarly, the radiative rate constants (k_f) calculated from ϕ_f/τ_f and the non-radiative rate constants (k_{nr}) obtained from $k_f(1/\phi_f - 1)$ remain unaffected by the solvent polarity. This behavior shows the absence of TICT states in polar solvent, as expected from the weak acceptor property of the ester function.

LB films with **1** and **2**

Fig. 5 shows the surface pressure–area (π - A) isotherms for monolayers of **1** and **2** while Table 3 collects the compression isotherm data for dyes **1–4**.¹⁶ For all compounds, the shape of the isotherms indicates good film-forming ability and no apparent phase transition during compression. Nevertheless, the π - A isotherms of **2–4** are more abrupt than for **1**, as reflected by the values of A_0 (see Table 3). The abrupt character of the **2–4** isotherms can be attributed to a molecule organization similar from the beginning to the end of monolayer for-

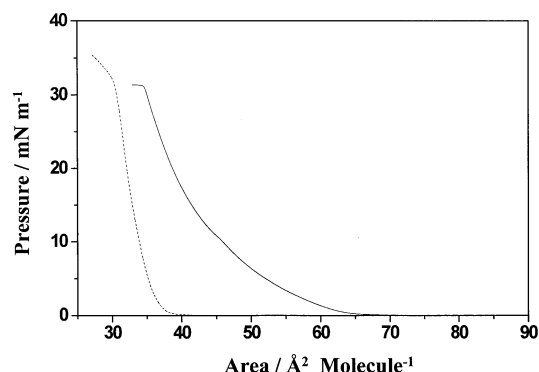


Fig. 5 Compression isotherm of Langmuir films at the air–water interface at room temperature for **1** (solid line) and **2** (dotted line).

Table 3 Compression isotherm data of monolayer LB films of **1–4**: absorption maxima ($\lambda_{\text{abs}}^{\text{max}}$) area per molecule at zero surface pressure (A_0), limiting area per molecule at the collapse point (A_c) and surface pressure of the collapse point (Π_c), wavelength of the titanium sapphire laser (λ_{exc}), molecular second harmonic hyperpolarizability (β) and average tilt angle (θ_0)

	1	2	3	4
$\lambda_{\text{abs}}^{\text{max}}/\text{nm}$	364	337	341	329
$A_0/\text{\AA}^2 \text{ molecule}^{-1}$	65	36	44	47
$A_c/\text{\AA}^2 \text{ molecule}^{-1}$	34	28	30	30
$\Pi_c/\text{mN m}^{-1}$	31	32	34	35
$\lambda_{\text{exc}}/\text{nm}$	800	800	788	788
$\beta/10^{-30} \text{ esu}^a$	300	290	200	190
θ_0/deg	32	32	32	31

^a esu = electrostatic unit; $\beta = 1 \text{ m}^4 \text{ V}^{-1} = 4.189 \times 10^{-10} \text{ esu}$.

mation, while the gradual behavior of **1** reflects different configurations involved during film formation.

From the π - A isotherms the collapse pressure (Π_c , Table 3) is estimated to be around 35 mN m^{-1} for **3** and **4** and 30 mN m^{-1} for **1** and **2**. This demonstrates a good stability of the LB films, as expected with perfluorinated chains. The lower stability recorded for **1** and **2** is directly related to the shorter length of the fluorinated chain. The limiting area per molecule, determined when the monolayer starts to collapse (A_c , Table 3), is close to the area of perfluoroundecanoic acid ($\text{C}_{10}\text{F}_{21}\text{COOH}$, $33.2 \text{ \AA}^2 \text{ molecule}^{-1}$)⁴⁶ but larger than the A_c values obtained for surfactant derivatives containing the *trans*-stilbene chromophore ($22 \text{ \AA}^2 \text{ molecule}^{-1}$)⁴⁷ and larger than the estimated value of the molecular cross-sectional area of the fluorocarbon chain (28 \AA^2).⁴⁸ This slight increase of the molecular cross-sectional area can reflect a tilted arrangement of the dyes in the LB films (see absorption and SHG measurements).

After stabilization of the Langmuir film, transfer is achieved at a constant pressure of 28 mN m^{-1} for **1** and 30 mN m^{-1} for **2**. The absorption spectra have been measured for an increasing number N of superposed monolayers (Fig. 6). For up to nine monolayers, the absorbance remains proportional to N , showing a regular organization in this LB film. Fig. 7 shows a comparison between the normalized absorption spectra of **2** in chloroform solution and as five superposed monolayers on a CaF_2 support. The absorption band of the LB film is wider and the maximum is blue-shifted. These changes in absorption spectra can be explained by the formation of aggregates. The proximity of the molecules in a LB film induces intermolecular interactions that affect both ground and excited state energies.¹⁴ Similar changes in the absorption spectra (hypsochromic shift) have been observed

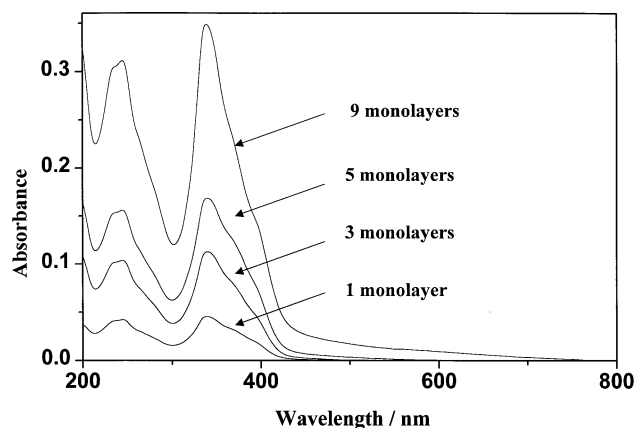


Fig. 6 Absorption spectra of LB films of **2** as a function of the number of layers.

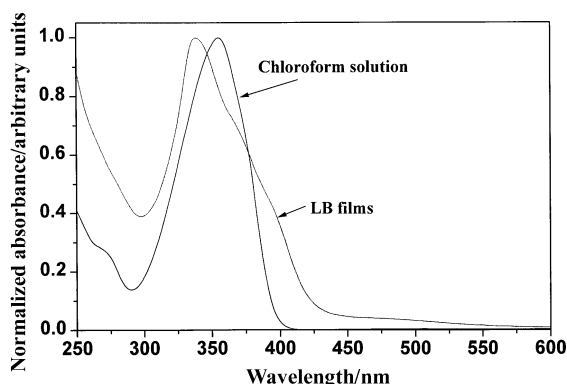


Fig. 7 Normalized absorbance spectra of **2** in chloroform and in LB Y-type multilayers (5 superposed monolayers) on a hydrophobic fluorine substrate.

for mono- and multi-layer LB films of *trans*-stilbene surfactants, containing nonpolar groups^{11,12} or p-donor and p'-acceptor substituents,¹³ even in dilute conditions.¹¹⁻¹³ This blue absorption shift was attributed to an H-aggregate arrangement in which the chromophore transition moments are aligned with an angle θ inferior to 36 degrees.^{12,13} In fact, a tilt angle larger than 36° induces a bathochromic shift of the absorption and is characteristic of J-aggregates, according to the model of Kasha *et al.*,¹⁴ as reported for 4-octadecylamino-4'-nitro stilbene.⁴⁹ In the case of **1** and **2**, the blue-shift of the absorption spectra (Fig. 7) suggests that H-aggregation is the predominant arrangement.

Second harmonic generation

For films of both **1** and **2**, the s-polarized component of the second harmonic signal, although measurable, is very weak for s- and p-polarized incident radiation. On the contrary, an intense signal is observed for the p-polarized component at 2ω for **1** and **2** when the incident beam is polarized either s or p. To obtain the average molecular orientation in the film and the second-order molecular polarizability we have followed the now classical method first proposed by Blombergen and Pershan⁵⁰ and subsequently refined by Shen.⁵¹ For stilbenes, only one component, $\alpha_{\xi\xi\xi}^{(2)} = \beta$, of the molecular second-order polarizability tensor is significant. The surface nonlinear susceptibility tensor $\chi^{(2)}$ is a function of $N\langle\alpha_{\xi\xi\xi}^{(2)}\rangle_f$, where N is the molecular surface density, ξ is the direction of the molecular dipole moment and f denotes the monolayer orientational distribution function. The ξ direction is approximately given by the donor-acceptor direction. In the xy plane (z axis normal to the substrate) only two distinct nonzero elements have to be taken into account: $\chi_{zzz}^{(2)}$ and $\chi_{zii}^{(2)} = \chi_{izi}^{(2)} = \chi_{iiz}^{(2)}$, where $i = x, y$. The average tilt angle θ_0 of the molecular axis can be estimated from $\chi_{zzz}^{(2)} (= N\alpha_{\xi\xi\xi}^{(2)} \cos^3 \theta_0)$ and $\chi_{zyy}^{(2)} (= (N/2)\alpha_{\xi\xi\xi}^{(2)} \sin^2 \theta_0 \cos \theta_0)$ with the assumption that the θ distribution is well peaked, that is, $f(\theta) = \delta(\theta - \theta_0)/\sin \theta_0$.

Our monolayer symmetry implies that the second-order s-polarized field is null: that is, $E^{s \rightarrow s}(2\omega) = E^{p \rightarrow s}(2\omega) = 0$. In this notation, ω is the frequency of the incident radiation, the first subscript indicates the polarization (s or p) of this incident radiation and the second subscript denotes the polarization (s or p) of the SH signal. The nonzero second-order p-polarized electric fields are proportional to the surface nonlinear tensor elements, as defined by eqn. (2) and (3), where the three constants A , B and C are related to the angle of incidence and to the dielectric indices of the glass substrate and of the film at ω and 2ω .

$$E^{s \rightarrow p}(2\omega) \propto A\chi_{zyy}^{(2)}[E^p(\omega)]^2 \quad (2)$$

$$E^{p \rightarrow p}(2\omega) \propto (B\chi_{zyy}^{(2)} + C\chi_{zzz}^{(2)})[E^p(\omega)]^2 \quad (3)$$

Table 3 collects the tilt angle θ_0 and the molecular second-order hyperpolarizability β found from the SHG experiment of deposited single monolayer LB films containing **1** and **2**. Data previously reported for **3** and **4** are also gathered in Table 3. The azimuthal tilt angle of 32° for **1** and **2** is consistent with the H-aggregate arrangement proposed according to our absorption data. The dipole moment direction of the molecules is certainly close to the long axis of the chromophores and as a result, the benzoic acid ethyl ester moieties of **1** and **2** are probably perpendicular to the substrate.

The β values of **1** and **2** arranged in monolayer LB films are estimated to be around 300×10^{-30} esu, close to the 200×10^{-30} esu found for **3** and **4**. This result opens interesting perspectives for the design of noncentrosymmetric multilayers containing alternatingly layers of **1-4**. Firstly, we elaborate Y-type multilayers containing an odd number of layers and, as expected, the SHG intensity is equivalent to that of the signal recorded for a single monolayer. This confirms a head-to-head organization of the Y-type multilayers.

Table 4 Intensity of the p-polarized component (N_{pp}) of the SHG signal in multilayer LB films constituted of N bilayers of **2/4**. The signal recorded for the quartz crystal is also reported

N	N_{pp}	$N_{pp}^{1/2}$
1	2400	49
2	13 000	114
4	50 000	224
Quartz crystal	2400	49

Then, we prepared bilayer LB films (Y-type structure, see Fig. 2) containing **1/3** or **2/4**. As expected, the SHG signal is not negligible and suggests a noncentrosymmetric arrangement with dipolar moments oriented in the same direction. The study of the different SHG components reveals in fact that the s-polarized component is not negligible for s- and p-polarized incident radiation. This behavior shows the absence of an in-plane isotropic molecular orientation within the bilayer LB films. For instance, one may consider that the transfer process fixes a preferential axis along which the bilayer could rearrange during the transfer. Such rearrangement may occur due to an imperfect match of the limiting area per molecule within the two LB films of the bilayer. If such a rearrangement happens, the bilayer would have a C_{1v} symmetry that would account for the observed phenomena. Note that if such a rearrangement is induced one would expect to observe a more pronounced effect for the **1/3** bilayer film.

Multilayer LB films based on one, two and four bilayers of **1/3** or **2/4** have been prepared. The SHG signals measured as a function of the number of **2/4** bilayers are collected in Table 4. As expected, the intensity of the p-polarized components increases with the number of layers. Moreover, the increase of the square root of N_{pp} is proportional to the number of layers, indicating a regular noncentrosymmetric arrangement at least up to four bilayers. Similar SHG measurements have been performed on multilayers constituted by **1/3**. Unfortunately, the p-polarized component remains unaffected by the number of bilayers. The organization of the **1/3** multilayers is certainly responsible for such behavior. This is therefore a clear indication that to preserve a good polar orientation within a single LB film the limiting area per molecule within the two LB films has to be as close as possible. In fact, according to our data and discarding any other contributions to the disorganization of the multilayer, a mismatch of about 10% in the area per molecule within the layers drastically and rapidly affects the multilayer arrangement.

Conclusion

A new family of organic molecules for SONLO, displaying an interesting compromise in terms of the nonlinearity/transparency trade-off, has been investigated. We have demonstrated that it was possible to form LB films of **1** and **2**. The observed changes in absorption have been explained by H-aggregation and a tilt angle θ_0 of ca. 32° was estimated by SHG measurements. A molecular quadratic hyperpolarizability β of 300×10^{-30} esu has been recorded for both **1** and **2** in LB films. Multilayer LB films containing both **1/3** or **2/4** have been prepared. The proportional increase of the SHG signal with the number of bilayers for **2/4** proves the regular organization of these LB films.

Experimental

Apparatus and methods

The course of the reactions and the purity of the final products were monitored by thin-layer chromatography (TLC). Melting points were determined on a Mettler FP 62 capillary

melting point apparatus and are uncorrected. ^1H NMR spectra were recorded on a Bruker AC 200 at 200 MHz or on a Bruker AC 250 spectrometer at 250 MHz. ^{13}C NMR spectra were recorded on a Bruker AC 250 spectrometer at 63 MHz. Infrared spectra were recorded on a Paragon 1000 Perkin–Elmer infrared spectrophotometer with polystyrene as standard (film on NaCl or dispersion in KBr).

Langmuir films of **1** and **2** were prepared under a constant nitrogen flow in a dark KSV 5000 double trough. Ultrapure water purified in a Milli-Q-System (Millipore) was used as subphase (resistivity 18.2 M Ω cm). Stock solution concentration was 10^{-3} mol l^{-1} in chloroform (Prolabo, HPLC grade) for **1** and in toluene containing 1% methanol (Prolabo, HPLC grade) for **2**. The compression was started 30 min after spreading of the solution (ca. 200 μl). The monolayer was compressed at room temperature at a barrier speed of 100 mm min^{-1} . Surface pressure was monitored with a Pt-Wilhelmy balance. The transfer on hydrophilic CaF_2 slides was realized under a constant pressure using a transfer speed of 1.75 mm min^{-1} . When several monolayers were superposed, the drying period between two depositions was set to 20 min under nitrogen. Alternating layers were prepared using a KSV 5000 double-trough according the same experimental conditions as described for the LB film formation. Transfer was realized on hydrophobic CaF_2 slides previously prepared by depositing three layers of behenic acid on hydrophilic slides and was performed at a surface pressure of 15 mN m^{-1} with a dipping and lifting speed of 5 mm min^{-1} .

Absorption and emission spectra were recorded on a Cary 5E spectrophotometer and Edinburgh Instruments spectrometer, respectively. Fluorescence spectra were recorded in quartz cells with right angle detection. Solvents were of spectroscopic quality. Fluorescence quantum yields were relative to **3** in diethyl ether ($\phi_f = 0.49$).¹⁷ Fluorescence decays of aerated solutions were measured using a single-photon-counting setup from Edinburgh Instruments.

The sapphire surface SHG measurements were made using a mode-locked titanium sapphire laser operating at a 76 MHz repetition rate and with a wavelength of 800 nm. The incident radiation, polarized parallel (p) or perpendicular (s) to the plane of incidence, was focused on the CaF_2 slide and directed at a 45° angle to the substrate normal.¹⁶ The SHG signal, resolved into s- and p-polarized components, was detected at 90° to the pumping direction by a photon-counting photomultiplier at the output of a monochromator. Sample regions free of any LB film exhibit no SHG. The SHG detected signal was calibrated against a properly oriented Z-cut quartz crystal.

Synthesis of **1**

(1H,1H,2H,2H-Perfluorooctyl)-3-methoxyphenylamine (6). 1H,1H,2H,2H-Perfluoro-1-iodooctane (10 g, 21.1 mmol) was added dropwise to 3-methoxyaniline (13 g, 105.5 mmol) at 90°C . After complete addition, the mixture was stirred at 140°C for 3 h (the reaction was monitored by GPC). After cooling, the organic layer was washed with 2 N aqueous sodium hydroxide (100 ml) and the aqueous layer extracted with diethyl ether (3×30 ml). Then, the organic layer was washed with water and dried with sodium sulfate. The solvent was removed under reduced pressure and the excess 3-methoxyaniline was distilled off under reduced pressure to give a brown residue. The crude product was purified by chromatography on a silica gel column eluting with dichloromethane to give the product **6** as a clear oil (9.7 g, 98%). δ_{H} (250 MHz, CDCl_3): 2.42 (m, 2H), 3.54 (m, 2H), 3.80 (s, 3H), 3.80 (s, 1H), 6.18–7.18 (m, 4H); δ_{C} (63 MHz, CDCl_3): 30.6 ($^2J_{\text{CF}} = 21.0$), 35.8 ($^3J_{\text{CF}} = 4.3$ Hz), 55.1, 99.0, 103.2, 105.9, 130.3, 148.3, 161.0; IR ν_{max} (cm^{-1}): 3409, 1675, 1515, 1240, 1145.

Ethyl[1*H*,1*H*,2*H*,2*H*-perfluorooctyl]-3-methoxyphenyl]-amine (7). Ethyl iodide (9.2 g, 58.8 mmol) was added dropwise to a stirred solution of **6** (6.9 g, 14.4 mmol), powdered sodium carbonate (6.2 g, 58.8 mmol) and acetone (20 ml) at room temperature. After complete addition, the mixture was refluxed for 72 h (the reaction was monitored by TLC). After cooling, the mixture was poured into water (50 ml) and standard ethereal work-up (3 × 40 ml) provided the crude amine, which was purified by chromatography on a silica gel column eluting with 40% petroleum ether in dichloromethane to give the product **7** as a clear oil (5.8 g, 80%). δ_{H} (250 MHz, CDCl₃): 1.20 (t, 3H, $^3J_{\text{HH}} = 7$), 2.39 (m, 2H, $^3J_{\text{HH}} = 8$, $^3J_{\text{HF}} = 19$), 3.38 (q, 2H, $^3J_{\text{HH}} = 7$ Hz), 3.66 (m, 2H), 3.80 (s, 3H), 6.25–7.24 (m, 4H); δ_{C} (63 MHz, CDCl₃): 12.4, 28.7 ($^2J_{\text{CF}} = 21.0$), 42.2 ($^3J_{\text{CF}} = 4.8$ Hz), 45.3, 55.0, 98.7, 101.4, 105.1, 130.3, 148.3, 161.2; IR ν_{max} (cm⁻¹): 1613, 1501, 1380, 1238, 1145.

3-[Ethyl(1*H*,1*H*,2*H*,2*H*-perfluorooctyl)amino]phenol (8). A 1.0 M boron tribromide solution in dichloromethane (22 ml, 22.2 mmol) was added dropwise to a stirred solution of **7** (5.1 g, 10.2 mmol) in dichloromethane (40 ml) at 0 °C. After complete addition, the reaction mixture was stirred for 24 h at room temperature. The mixture was poured into ice-cold water, then extracted with dichloromethane (3 × 40 ml) and dried with magnesium sulfate. Removal of solvent gave a purple oily residue, which was purified by chromatography on a silica gel column eluting with 30% petroleum ether in dichloromethane to give the product **8** as an orange oil (3.1 g, 63%). δ_{H} (200 MHz, CDCl₃): 1.22 (t, 3H, $^3J_{\text{HH}} = 7.1$), 2.40 (m, 2H, $^3J_{\text{HH}} = 7.8$, $^3J_{\text{HF}} = 19.9$), 3.39 (q, 2H, $^3J_{\text{HH}} = 7.1$ Hz), 3.67 (m, 2H), 5.04 (s, 1H), 6.23–7.30 (m, 4H); δ_{C} (50 MHz, CDCl₃): 12.4, 28.7 ($^2J_{\text{CF}} = 21.7$ Hz), 42.1, 45.2, 99.1, 103.7, 104.8, 130.5, 148.5, 156.9; IR ν_{max} (cm⁻¹): 3361, 1614, 1504, 1384, 1205, 1144.

2-Hydroxy-4-[ethyl(1*H*,1*H*,2*H*,2*H*-perfluorooctyl)-amino]benzaldehyde (9). A mixture of dimethylformamide (4 g, 54.3 mmol) and phosphorus oxychloride (0.8 g, 5.2 mmol) was stirred at 0 °C for 1 h under nitrogen atmosphere, then at room temperature for 1.5 h to give an orange solution. The latter was cannulated into a mixture of **8** (2.5 g, 5.2 mmol) and dimethylformamide (1 ml). The resulting solution was stirred at 95 °C for 15 h. After cooling, the reaction mixture was poured into ice-cold water, washed with aqueous sodium hydroxide (10%) and the aqueous layer was extracted with dichloromethane (3 × 50 ml). The organic layer was washed with water (3 × 30 ml) and dried with magnesium sulfate. Removal of the solvent gave a red oil, which was purified by chromatography on a silica gel column eluting with 30% petroleum ether in dichloromethane to give the product **9** as a grey solid (1 g, 38%). Mp 68–69 °C; δ_{H} (250 MHz, CDCl₃): 1.22 (m, 2H, $^3J_{\text{HH}} = 7.1$), 2.36 (tt, 2H, $^3J_{\text{HH}} = 8.1$, $^3J_{\text{HF}} = 20.2$), 3.40 (q, 2H, $^3J_{\text{HH}} = 7.1$ Hz), 3.68 (m, 2H), 6.08–6.31 (m, 3H), 9.51 (s, 1H, CHO), 10.54 (s, 1H, OH); δ_{C} (50 MHz, CDCl₃): 12.4, 28.8 ($^2J_{\text{CF}} = 21.8$ Hz), 42.3, 45.4, 97.2, 104.1, 112.2, 135.7, 153.5, 164.4, 192.6; IR ν_{max} (cm⁻¹): 1636, 1519, 1344, 1235, 1186.

4-Bromomethylbenzoic acid ethyl ester (11). A well-stirred mixture of 4-methylbenzoic acid ethyl ester **10** (1.2 g, 7.3 mmol), *N*-bromosuccinimide (1.4 g, 7.8 mmol) and benzoyl peroxide (20 mg) in dry carbon tetrachloride (15 ml) was refluxed for 15 h. The hot mixture was filtered and the filtrate was evaporated to give a white residue, which was purified by chromatography on a silica gel column eluting with 30% dichloromethane in petroleum ether to give the product **11** as a colorless oil (1.1 g, 67%). δ_{H} (200 MHz, CDCl₃): 1.36 (t, 3H, $^3J_{\text{HH}} = 7.1$), 4.35 (q, 2H, $^3J_{\text{HH}} = 7.1$ Hz), 4.46 (m, 2H), 7.39, 7.43, 7.97, 8.01 (AA'BB', 4H); δ_{C} (50 MHz, CDCl₃): 14.0, 32.0, 60.8, 128.7, 129.7, 130.1, 142.2, 165.6; IR ν_{max} (cm⁻¹): 1716, 1611, 1278, 1108.

4-{2-Formyl-5-[ethyl(1*H*,1*H*,2*H*,2*H*-perfluorooctyl)-amino]phenoxyethyl}benzoic acid ethyl ester (12). A solution of **9** (686 mg, 1.34 mmol), **11** (373 mg, 1.53 mmol) and powdered potassium carbonate (0.5 mg, 3.62 mmol) in dimethylformamide (10 ml) was stirred at 100 °C for 20 h. After cooling, the solvent was eliminated under reduced pressure and water (50 ml) was added. The aqueous phase was separated, extracted with dichloromethane, washed with water and dried over magnesium sulfate. Chromatography on a silica gel column eluting with dichloromethane gave **12** as a red solid (366 mg, 40%). Mp 101 °C; δ_{H} (250 MHz, CDCl₃): 1.17 (t, 3H, $^3J_{\text{HH}} = 7.0$), 1.39 (t, 3H, $^3J_{\text{HH}} = 7.2$), 2.33 (m, 2H), 3.40 (q, 2H, $^3J_{\text{HH}} = 7$), 3.64 (m, 2H), 4.37 (q, 3H, $^3J_{\text{HH}} = 7.2$ Hz) 5.2 (s, 2H), 6.0–7.7 (m, 3H), 7.47, 7.51, 8.05, 8.08 (AA'BB', 4H), 10.3 (s, 1H); δ_{C} (63 MHz, CDCl₃): 12.4, 45.5, 69.4, 28.7 ($^2J_{\text{CF}} = 21.0$ Hz), 42.3 ($^3J_{\text{CF}} = 5.7$ Hz), 14.3, 61.1, 94.5, 104.6, 115.4, 126.5, 130.0, 130.3, 131.0, 141.4, 152.8, 162.8, 166.2, 187.2; IR ν_{max} (cm⁻¹): 1708, 1598, 1518, 1238, 1140.

4-{6-[Ethyl(1*H*,1*H*,2*H*,2*H*-perfluorooctyl)amino]-benzofuran-2-yl}benzoic acid ethyl ester (1). The reagent potassium fluoride/alumina was first prepared according to the following procedure. Potassium fluoride (4 g, 68.84 mmol) was mixed with alumina (6 g) in water (20 ml) for 1 h. Water was removed in a rotary evaporator and the impregnated alumina was dried under vacuum at 80 °C for 12 h. A solution of **12** (530 mg, 0.8 mmol) and powdered potassium fluoride/alumina (1.2 g, 0.79 mmol), in dimethylformamide (5 ml) was stirred at 120 °C for 4 h (the reaction was monitored by TLC). After cooling, the solid material was filtered off and washed with ether. Removal of solvent under reduced pressure gave a yellow-brown oily residue. The product was purified by column chromatography on silica gel eluting with dichloromethane to give **1** as a yellow solid (144 mg, 24%). Mp 110 °C; δ_{H} (250 MHz, CDCl₃): 1.17 (t, 3H, $^3J_{\text{HH}} = 7.0$), 1.35 (t, 3H, $^3J_{\text{HH}} = 7.2$), 2.35 (m, 2H), 3.37 (q, 2H, $^3J_{\text{HH}} = 7.0$), 3.66 (m, 2H), 4.33 (q, 3H, $^3J_{\text{HH}} = 7.2$ Hz), 6.97 (s, 1H), 6.65–7.39 (m, 3H), 7.83, 7.86, 8.07, 8.10 (AA'BB', 4H); δ_{C} (63 MHz, CDCl₃): 12.5, 14.4, 28.3 ($^2J_{\text{CF}} = 21.0$), 61.0, 42.8 ($^3J_{\text{CF}} = 5.7$ Hz), 45.9, 94.6, 103.8, 110.1, 119.5, 121.8, 123.8, 129.1, 130.1, 134.8, 145.9, 152.8, 157.4, 166.4; IR ν_{max} (cm⁻¹): 1708, 1606, 1503, 1381, 1271, 1139; MS (EI) *m/z*: 655 (M⁺, 100), 222 (M⁺ – CH₂C₆F₁₃, 10).

Synthesis of 2

(1*H*,1*H*,2*H*,2*H*-Perfluorooctyl)phenylamine (14). 1*H*,1*H*,2*H*,2*H*-Perfluoro-1-iodooctane (20.4 g, 43 mmol) was added dropwise to aniline (16 g, 171.8 mmol) at 90 °C. After complete addition, the mixture was stirred at 140 °C for 15 h (the reaction was monitored by GPC). After cooling, the organic layer was washed with 2 N aqueous sodium hydroxide (100 ml) and the aqueous layer extracted with diethyl ether (3 × 40 ml). Then, the organic layer was washed with water and dried with magnesium sulfate. Solvent was removed under reduced pressure and the residue was purified by distillation, bp_{0.0026 atm} 116–117 °C, to give the product **14** as a clear colorless liquid (15.9 g, 85%). δ_{H} (250 MHz, CDCl₃): 2.42 (tt, 2H, $^3J_{\text{HH}} = 7.1$, $^3J_{\text{HF}} = 18.8$), 3.57 (t, 2H, $^3J_{\text{HH}} = 7.1$ Hz), 3.77 (s, 1H), 6.64–7.29 (m, 5H); δ_{C} (63 MHz, CDCl₃): 30.7 ($^2J_{\text{HF}} = 20.0$ Hz), 35.8, 112.9, 118.8, 129.6, 146.9; IR ν_{max} (cm⁻¹): 3417, 1605, 1510, 1365, 1240, 1145.

Methyl[(1*H*,1*H*,2*H*,2*H*-perfluorooctyl)phenyl]amine (15). Methyl iodide (5.9 g, 41.5 mmol) was added dropwise to a stirred solution of **14** (10 g, 22.8 mmol), powdered sodium carbonate (2.5 g, 23 mmol) and acetone (20 ml) at room temperature. After complete addition, the mixture was refluxed for 72 h (the reaction was monitored by GPC). After cooling, the mixture was poured onto water (70 ml), the organic layer separated and the aqueous phase extracted with dichloro-

methane (3 × 40 ml). The organic phase was washed with water and dried with magnesium sulfate. Solvent was removed under reduced pressure to give a residue, which was purified by chromatography on a silica gel column eluting with 40% dichloromethane in petroleum ether to give the product **15** as a clear colorless liquid (9 g, 85%). δ_{H} (250 MHz, CDCl_3): 2.36 (tt, 2H, $^3J_{\text{HH}} = 7.6$, $^3J_{\text{HF}} = 19.0$), 2.98 (s, 3H), 3.74 (t, 2H, $^3J_{\text{HH}} = 7.6$ Hz), 6.73–7.33 (m, 5H); δ_{C} (50 MHz, CDCl_3): 27.5 ($^2J_{\text{CF}} = 21.8$ Hz), 38.2, 44.3, 112.3, 117.2, 129.5, 148.0; IR ν_{max} (cm^{-1}): 1602, 1508, 1365, 1240, 1145.

4-[Methyl(1H,1H,2H,2H-perfluorooctyl)amino]-benzaldehyde (16). A mixture of dimethylformamide (5.1 g, 70.4 mmol) and phosphorus oxychloride (3.1 g, 19.4 mmol) was stirred at 0 °C for 1.75 h under a nitrogen atmosphere, then at room temperature for 1.25 h to give an orange solution. To the resulting solution, **15** (8 g, 17.6 mmol) was added dropwise and the resulting mixture was stirred at 100 °C for 15 h. After cooling, the reaction mixture was poured into ice-cold water (50 ml), washed with 2 N aqueous sodium hydroxide (10%), the organic layer was separated and the aqueous layer extracted with dichloromethane (4 × 50 ml). The organic layer was washed with water (3 × 25 ml) and dried with magnesium sulfate. Removal of the solvent under reduced pressure gave a brown oily residue, which was purified by chromatography on a silica gel column eluting with 20% petroleum ether in dichloromethane to give the product **16** as a pale yellow solid (7 g, 80%). Mp 44 °C; δ_{H} (250 MHz, CDCl_3): 2.35 (tt, 2H, $^3J_{\text{HH}} = 7.5$, $^3J_{\text{HF}} = 18.8$), 3.06 (s, 3H), 3.76 (t, 2H, $^3J_{\text{HH}} = 7.5$ Hz), 6.67, 6.71, 7.72, 7.75 (AA'BB', 4H), 9.91 (s, 1H); δ_{C} (63 MHz, CDCl_3): 27.9 ($^2J_{\text{CF}} = 22.0$ Hz), 38.4, 44.3, 111.1, 126.1, 132.2, 152.4, 190.3; IR ν_{max} (cm^{-1}): 1683, 1593, 1527, 1383, 1240, 1164.

3-Nitro-4-methylbenzoyl chloride (18). 3-Nitro-4-methylbenzoic acid (10 g, 55.2 mmol) was added in small amounts to thionyl chloride (50 g, 420 mmol) at room temperature. After the addition, the solution was refluxed for 3 h. The excess of thionyl chloride was removed under reduced pressure and the solution azeotroped with toluene (3 × 100 ml) to give the benzoyl chloride **18** as a pale green oil (11.2 g, quantitative yield); the product was used without further purification. δ_{H} (250 MHz, CDCl_3): 2.67 (s, 3H), 7.46 (d, 1H, $^3J_{\text{HH}} = 8.1$), 8.16 (dd, 1H, $^3J_{\text{HH}} = 8.1$, $^4J_{\text{HH}} = 1.9$), 8.65 (d, 1H, $^4J_{\text{HH}} = 1.8$ Hz); δ_{C} (63 MHz, CDCl_3): 20.8, 127.2, 132.2, 133.6, 134.2, 141.1, 150.1, 167.2.

3-Nitro-4-methylbenzoic acid ethyl ester (19). Ethanol (40 ml) was added dropwise to **18** (11 g, 54 mmol) at room temperature. After complete addition, the solution was refluxed for 8 h. The excess of ethanol was removed under reduced pressure. The residue was dried under vacuum and was purified by chromatography on a silica gel column eluting with dichloromethane to give the product **19** as a colorless oil (10.7 g, 95%). δ_{H} (250 MHz, CDCl_3): 1.38 (t, 3H, $^3J_{\text{HH}} = 7.1$), 2.62 (s, 3H), 4.38 (q, 2H, $^3J_{\text{HH}} = 7.1$), 7.40 (d, 1H, $^3J_{\text{HH}} = 8.0$), 8.11 (dd, 1H, $^3J_{\text{HH}} = 8.0$, $^4J_{\text{HH}} = 1.7$), 8.54 (d, 1H, $^4J_{\text{HH}} = 1.7$ Hz); δ_{C} (63 MHz, CDCl_3): 14.2, 20.5, 61.6, 125.7, 129.7, 132.9, 133.3, 138.2, 149.8, 164.4; IR ν_{max} (cm^{-1}): 1720, 1535, 1347, 1290, 1265.

4-Bromomethyl-3-nitrobenzoic acid ethyl ester (20). A well-stirred mixture of **19** (5 g, 23.9 mmol), *N*-bromosuccinimide (4.2 g, 23.9 mmol) and benzoyl peroxide (20 mg) in dry carbon tetrachloride (45 ml) was refluxed for 15 h. The hot mixture was filtered and the filtrate was evaporated to give a white solid residue, which was purified by chromatography on a silica gel column eluting with 25% dichloromethane in petroleum ether to give the product **20** as a yellow solid (4.1 g, 60%). Mp 43 °C; δ_{H} (250 MHz, CDCl_3): 1.35 (t, 3H, $^3J_{\text{HH}} = 7.1$), 4.36 (q, 2H, $^3J_{\text{HH}} = 7.1$), 4.77 (s, 2H), 7.60 (d, 1H, $^3J_{\text{HH}} =$

8.0), 8.17 (dd, 1H, $^3J_{\text{HH}} = 8.0$, $^4J_{\text{HH}} = 1.6$), 8.57 (d, 1H, $^4J_{\text{HH}} = 1.6$ Hz); δ_{C} (63 MHz, CDCl_3): 14.2, 27.9, 62.1, 126.4, 132.0, 132.7, 134.1, 136.9, 148.5, 164.5; IR ν_{max} (cm^{-1}): 1720, 1535, 1347, 1290, 1265.

(4-Ethoxycarbonyl-2-nitrobenzyl)triphenylphosphonium bromide (21). A solution of **20** (1.8 g, 6.2 mmol) and triphenylphosphine (1.9 g, 7.2 mmol) in dry toluene (25 ml) was stirred at 110 °C for 16 h. After cooling, the product was filtered off and evaporated to dryness to give the phosphonium salt as a pale brown solid (3.1 g, 91%). Mp 197 °C; δ_{H} (250 MHz, CDCl_3): 1.31 (t, 3H, $^3J_{\text{HH}} = 7.1$), 4.32 (q, 2H, $^3J_{\text{HH}} = 7.1$), 6.06 (s, 2H, $^2J_{\text{HP}^+} = 15.3$ Hz), 7.55–7.78 (m, 15H), 8.11 (AB, 2H), 8.44 (s, 1H); δ_{C} (63 MHz, CDCl_3): 13.9, 28.3 ($^1J_{\text{CP}^+} = 48.7$ Hz), 61.9, 126–137 (18 C_{H} , 2 C_{q}), 163.7; IR ν_{max} (cm^{-1}): 1718, 1536, 1438, 1300, 1268, 1110.

4-[Methyl(1H,1H,2H,2H-perfluorooctyl)amino]-2-nitro-trans-stilbene-4-carboxylic acid ethyl ester (22). A mixture of **16** (2.6 g, 5.4 mmol), **21** (3 g, 5.4 mmol) and powdered potassium carbonate (1.6 g, 11.5 mmol) in dimethylformamide (20 ml) was stirred at 90 °C for 20 h. After cooling, the excess of dimethylformamide was removed under vacuum and water (50 ml) was added. The aqueous layer was extracted with dichloromethane (3 × 50 ml); the organic layer was washed with water (3 × 25 ml) and dried with magnesium sulfate. Removal of the solvent under reduced pressure gave a red solid residue. This was purified by chromatography on a silica gel column eluting with 30% petroleum ether in dichloromethane to give **22** as a red solid (1.5 g, 40%). Mp 105–106 °C; δ_{H} (250 MHz, CDCl_3): 1.42 (t, 3H, $^3J_{\text{HH}} = 7.1$); 2.37 (m, 2H, $^3J_{\text{HH}} = 7.3$, $^3J_{\text{HF}} = 19.0$); 3.03 (s, 3H); 3.75 (t, 2H, $^3J_{\text{HH}} = 7.3$), 4.42 (q, 2H, $^3J_{\text{HH}} = 7.1$), 6.68, 6.71, 7.46, 7.49 (AA'BB', 4H), 7.18 (d, 1H, $^3J_{\text{HHtrans}} = 16$), 7.42 (d, 1H, $^3J_{\text{HHtrans}} = 16$ Hz), 8.54 (s, 1H); δ_{C} (63 MHz, CDCl_3): 14.3, 27.7 ($^2J_{\text{CF}} = 22$ Hz), 38.3, 44.4, 61.7, 112.1, 117.8, 125.1, 126.2, 127.2, 129.0, 129.2, 133.1, 136.1, 137.3, 147.4, 148.6, 164.6.

2-{4-[Methyl(1H,1H,2H,2H-perfluorooctyl)amino]phenyl}-1H-indole-6-carboxylic acid ethyl ester (2). A mixture of **22** (1 g, 1.5 mmol) and triethyl phosphite (10 ml) was refluxed for 18 h. After cooling, the excess of triethyl phosphite was removed by distillation (bp 156–157 °C). Water (30 ml) was added, the organic layer separated and the aqueous layer was extracted with diethyl ether (3 × 30 ml). The organic layer was washed with water (10 ml) and dried with magnesium sulfate. Removal of the solvent under reduced pressure gave an orange solid residue. This was reprecipitated by adding dichloromethane to give the product **2** as a yellow solid (0.1 g, 10%). Mp 212 °C; δ_{H} (200 MHz, acetone- d_6): 1.40 (t, 3H, $^3J_{\text{HH}} = 7.1$), 2.60 (m, 2H, $^3J_{\text{HH}} = 7.3$, $^3J_{\text{HF}} = 20.1$), 3.12 (s, 3H), 3.91 (t, 2H, $^3J_{\text{HH}} = 7.3$), 4.36 (q, 2H, $^3J_{\text{HH}} = 7.1$ Hz), 6.91, 6.95, 7.79, 7.83 (AA'BB', 4H), 6.84–8.12 (m, 4H), 10.83 (s, 1H); δ_{C} (63 MHz, acetone- d_6): 14.7, 30.1, 38.3, 44.4, 60.8, 98.8, 113.3, 113.6, 119.8, 121.4, 123.5, 126.9, 127.6, 132.9, 137.1, 137.8, 144.1, 167.3; IR ν_{max} (cm^{-1}): 3365, 1689, 1610, 1506, 1369, 1233, 1189; MS (EI) *m/z*: 640 (M^+ , 100), 307 ($\text{M}^+ - \text{CH}_2\text{C}_6\text{F}_{13}$, 13).

References

- 1 J. L. Oudar, *J. Chem. Phys.*, 1977, **67**, 446.
- 2 J. F. Nicoud and R. Tveig, in *Nonlinear Optical Properties of Organic Molecules and Crystals*, eds. D. S. Chemla and J. Zyss, Academic Press, New York, 1987, p. 227.
- 3 *Molecular Nonlinear Optics: Materials, Physics, and Devices*, ed. J. Zyss, Academic Press, Boston, 1993.
- 4 D. M. Burland, R. D. Miller and C. A. Walsh, *Chem. Rev.*, 1994, **94**, 31.
- 5 T. J. Marks and M. A. Ratner, *Angew. Chem., Int. Ed. Engl.*, 1995, **34**, 155.

- 6 C. Sanchez and B. Lebeau, *Pure Appl. Opt.*, 1996, **5**, 689.
7 L. T. Cheng, W. Tam and A. E. Feiring, *Mol. Cryst. Liq. Cryst. Sci. Technol., Sect. B: Nonlinear Optics*, 1992, **3**, 69–71.
8 A. Ulman, C. S. Willand, W. Köhler, D. R. Robello, D. J. Williams and L. Handley, *J. Am. Chem. Soc.*, 1990, **112**, 7085.
9 J.-F. Létard, R. Lapouyade and W. Rettig, *J. Am. Chem. Soc.*, 1993, **115**, 2441.
10 R. Lapouyade, A. Kuhn, J.-F. Létard and W. Rettig, *Chem. Phys. Lett.*, 1993, **208**, 48.
11 E. M. Kosower, *Physical Organic Chemistry*, Wiley, New York, 1968.
12 W. F. Mooney, III and D. G. Whitten, *J. Am. Chem. Soc.*, 1986, **108**, 5712.
13 I. Furman, H. C. Geiger, D. G. Whitten, T. L. Penner and A. Ulman, *Langmuir*, 1994, **10**, 837.
14 M. Kasha, H. R. Rawls and M. A. El-Bayoumi, *Pure Appl. Chem.*, 1965, **11**, 371.
15 H. Le Breton, B. Bennetau, J. Dunoguès, J.-F. Létard, R. Lapouyade, L. Vignau and J.-P. Morand, *Langmuir*, 1995, **11**, 1353.
16 H. Le Breton, J.-F. Létard, R. Lapouyade, A. Le Calvez, R. Maleck Rassoul, E. Freysz, A. Ducasse, C. Belin and J.-P. Morand, *Chem. Phys. Lett.*, 1995, **242**, 604.
17 H. Le Breton, B. Bennetau, J.-F. Létard, R. Lapouyade and W. Rettig, *J. Photochem. Photobiol. A: Chem.*, 1996, **95**, 7.
18 J. Hoepken and M. Moeller, *Macromolecules*, 1992, **25**, 2482.
19 J. Zyss, *J. Mol. Electron.*, 1985, **1**, 25.
20 S. Ma, X. Lu, W. Wang and Z. Zhang, *J. Phys. D*, 1997, **30**, 2651.
21 G. J. Ashwell, *J. Mater. Chem.*, 1999, **9**, 1991.
22 I. Ledoux, D. Josse, J. Zyss, T. McLean, P. F. Gordon, R. A. Hann and S. Allen, *J. Chim. Phys.*, 1988, **85**, 1085.
23 E. Campaigne and W. L. Archer, *Org. Synth.*, 1953, **33**, 27.
24 E. Campaigne and W. L. Archer, *J. Am. Chem. Soc.*, 1953, **75**, 989.
25 G. Gryniewicz, M. Poenie and R. Y. Tsien, *J. Biol. Chem.*, 1985, **260**, 3440.
26 J. Yamawari, T. Kawate, T. Ando and T. Hanafusa, *Bull. Chem. Soc. Jpn.*, 1983, **56**, 1885.
27 R. Sureau and J. Pechmeze, *Ger. Pat.*, 2.353.293, 1974.
28 B. E. Maryanoff and A. B. Reitz, *Chem. Rev.*, 1989, **89**, 863.
29 R. J. Sundberg, *J. Org. Chem.*, 1973, **30**, 3604.
30 Y. Ooshika, *J. Phys. Soc. Jpn.*, 1954, **9**, 594.
31 E. Lippert, *Z. Naturforsch. A*, 1955, **10**, 541.
32 W. Liptay, *Z. Naturforsch. A*, 1965, **20**, 1441.
33 N. Mataga, Y. Kaifu and M. Koizumi, *Bull. Chem. Soc. Jpn.*, 1956, **29**, 465.
34 L. Onsager, *J. Am. Chem. Soc.*, 1936, **58**, 1486.
35 P. Suppan, *Chem. Phys. Lett.*, 1983, **94**, 272.
36 W. Baumann, H. Bischof, J. C. Fröhling, C. Brittinger, W. Rettig and K. Kotkiewicz, *J. Photochem. Photobiol. A: Chem.*, 1992, **64**, 49.
37 Cerius² Quantum Mechanics, Chemistry, MOPAC, AM1 Hamiltonian approximation method. Molecular Simulations Inc., San Diego, CA, USA, 1998.
38 W. Rettig and W. Majenz, *Chem. Phys. Lett.*, 1989, **154**, 335.
39 W. Rettig, W. Majenz, R. Lapouyade and G. Haucke, *J. Photochem. Photobiol. A: Chem.*, 1992, **62**, 415.
40 R. Lapouyade, K. Czeschka, W. Majenz, W. Rettig, E. Gilabert and C. Rullière, *J. Phys. Chem.*, 1992, **96**, 9643.
41 K. Rotkiewicz, K. H. Grellmann and Z. R. Grabowski, *Chem. Phys. Lett.*, 1973, **19**, 315; K. Rotkiewicz, K. H. Grellmann and Z. R. Grabowski, *Chem. Phys. Lett.*, 1973, **21**, 212 (erratum).
42 J.-F. Létard, R. Lapouyade and W. Rettig, *Chem. Phys. Lett.*, 1994, **222**, 209.
43 R. Lapouyade, A. Kuhn, J.-F. Létard and W. Rettig, *Chem. Phys. Lett.*, 1993, **208**, 48.
44 H. Ephardt and P. Fromherz, *J. Phys. Chem.*, 1989, **93**, 7717; H. Ephardt and P. Fromherz, *J. Phys. Chem.*, 1991, **95**, 6792.
45 P. Fromherz and A. Heilemann, *J. Phys. Chem.*, 1992, **96**, 6864.
46 H. Nakahama, S. Miyata, T. T. Wang and S. Tasaka, *Thin Solid Films*, 1986, **141**, 165.
47 S. P. Spooner and D. G. Whitten, *J. Am. Chem. Soc.*, 1994, **116**, 1240.
48 A. Laschewsky, H. Ringsdorf and G. Schmidt, *Thin Solid Films*, 1985, **134**, 153.
49 M. E. Lippitsch, S. Draxler and E. Koller, *Thin Solid Films*, 1992, **217**, 161.
50 N. Blombergen and P. S. Pershan, *Phys. Rev.*, 1962, **128**, 606.
51 Y. R. Shen, *Annu. Rev. Phys. Chem.*, 1989, **40**, 327.